Airborne Mineral Dust

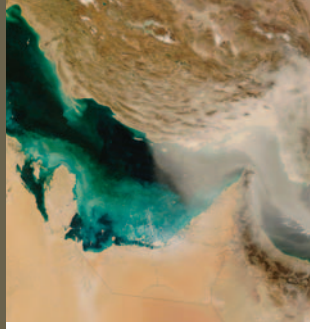

Johann P. Engelbrecht[1] and Edward Derbyshire[2]

1811-5209/10/0006-0241$2.50 DOI: 10.2113/gselements.6.4.241

Global dust events have been part of much of Earth's history. As in the geological past, mineral dust deflated off weathered crustal material in arid regions is continually being lofted kilometres into the atmosphere, where it circles the globe until physical and chemical processes favour precipitation in the ocean or on land. Mineral dust aerosols affect the environment both directly and indirectly by impacting the chemical and physical properties of the atmosphere and by interfering with biogeochemical cycles, all on a global scale. The most important source regions of dust are all in the Northern Hemisphere and include North Africa, the Middle East, the northwestern Indian subcontinent, central Asia, and northwestern China.

KEYWORDS: mineral dust, dust sources, dust pathways, dust fluxes

INTRODUCTION

Sources of dust, including tephra, occur globally, but the major source regions lie in and around the extremely arid to semi-arid drylands of the world (Prospero 1999). The largest of these stretches over 10,000 km, from the western Sahara in North Africa, through the Middle East, to central and eastern Asia.

Sources of erodible natural dust are found in wadis, salt pans, and alluvial deposits, as well as in ephemeral, saline, and dried out lakes (*playas*) throughout North Africa, the Middle East, the northwestern Indian subcontinent, central Asia (from the Caspian Sea to Kazakhstan), and northwestern China. Based on numerical simulation, Tanaka and Chiba (2006) concluded that North Africa is the largest single source region of dust on Earth, providing 58 wt% of total dust emissions, followed by the Arabian peninsula (12%), eastern China (8%) and central Asia (7%). Notable Southern Hemisphere source regions are Australia (6%), southern Africa (3%) and South America (2%). The western United States contributes ~0.1 wt% to the global dust flux.

The extent to which particles are taken up (deflated) from the ground surface depends on several factors: the critical wind speed necessary to dislodge particles (known as the threshold velocity); the instability of the atmosphere; particle size; the roughness and moisture content of the land surface; the degree of particle exposure; vegetation cover; and the mineralogical composition of loose dust on the ground surface.

1 Division of Atmospheric Sciences
Desert Research Institute
2215 Raggio Parkway
Reno, NV 89512-1095, USA
E-mail: Johann.Engelbrecht@dri.edu

2 The Grange,
Grange Court,
Aldwick, Bognor Regis,
West Sussex PO21 4XR, UK
E-mail: edwardderbyshire@btopenworld.com

Human activities (e.g. agriculture, deforestation, traffic on dirt roads) also generate substantial amounts of mineral dust. Anthropogenically disturbed land can become major dust sources, especially in the drought-stricken agricultural regions of Africa, Australia, China, and the Midwest of the USA. Past estimates of the magnitude of anthropogenic contributions to global dust load range from less than 10 to 50 wt%, a range of variation that reflects modelling uncertainties and a dearth of measured observational data. More recently, however, direct measurement by satellite-borne spectroradiometers combined with surface land-use data (Ginoux et al. 2010) shows that, in regions where between 5 and 25% of the land surface is disturbed, more than half the territory is potentially an anthropogenic dust source.

Mineral dust is composed of variable amounts of quartz, feldspars (plagioclase and alkali feldspar), micas (mainly muscovite and biotite), various clay minerals (illite, montmorillonite, palygorskite, kaolinite), carbonates (mostly calcite and dolomite), oxides (e.g. hematite, magnetite, rutile) and evaporite minerals (halite, gypsum, potassium sulphate). Minerals in dust occur as individual grains, aggregates or surface coatings – from less than 1 micrometre to ~30 micrometres (μm) in diameter.

Dust entrainment by saltation and suspension processes takes place mostly when winds are strong and gusty. Freshly entrained dust may initially have a mineral composition similar to that of the surface soil. Particle segregation and deposition of coarse material takes place over short distances, depending on the mineralogical composition and the physical properties of the dust. Fine and low-density particles remain in suspension and are lofted into the upper troposphere, where they circle the globe. Airborne dust also carries microfauna, including diatoms, bacteria and viruses; some of the latter remain alive despite being transported for distances of several thousand kilometres (Griffin 2007). African dust outbreaks are partly responsible for exceeding the maximum particle concentrations permitted by the particulate-matter guidelines in southern Europe.

HISTORICAL RECORDS

An indication of global dust flux on a geological timescale is provided by estimated accumulation rates of loess – wind-lain mineral dust – during the past 2.6 million years. Quasi-continuous accumulations of loess on continental drylands may contain evidence of changes in climate linked to

varying volumes of global ice (glacial and interglacial periods). Across the Chinese Loess Plateau (CLP), present mass accumulation rates (MARs) vary between ~25 and >500 g/m^2/y (Sun et al. 2000), and mean estimated MARs for the last interglacial period are broadly similar. However, average MARs for the last glacial period are between 2 and 4 times these values (Kohfeld and Harrison 2003). Ancient loess and modern dust deposits have broadly similar bulk compositions, although isotope signatures of neodymium (Nd) and strontium (Sr) indicate that the CLP deposits are dominated by dust from the northern margin of the Tibetan Plateau, which accords with the view that a strong link exists between this source and the CLP sink (e.g. Derbyshire et al. 1998). Long-range spring dust in both southern China (Nanjing) and Japan has Nd and Sr isotope compositions similar to those of loess. However, spring dust in northern China (Beijing) has a much lower Nd isotope ratio ($\varepsilon_{Nd}{}^0$), indicating an additional contribution of low-value $\varepsilon_{Nd}{}^0$ material, possibly from the sandy lands to the north and west (Li et al. 2009). Loess is prone to erosion by wind and water and to mass collapse. Thus, the world's thick loess deposits are important sources of resuspended mineral dust.

Antarctic and Greenland ice cores provide a stratigraphic record of both crustal and extraterrestrial dust. Mineral dust particles act as nuclei for ice crystallites that deposit as snow, which accumulates to become glaciers and ice sheets in high-mountain and polar regions. Dust concentrations in some ice cores are about two orders of magnitude higher during glacial periods than in interglacials, because the extent of dry land and desert terrain increases at times of lower sea levels (EPICA community members 2004). Similarly, cores of deep-sea and other marine sediments contain dust layers, evidence of past climatic changes (Jickells et al. 1998).

The *Iliad*, an example of early classical Greek literature written in the 8th century BCE and attributed to Homer, mentions "rain of blood" events. This phenomenon was interpreted later by Roman historians and philosophers, such as Cicero, Livy and Pliny, as raindrops contaminated by red clay from a terrestrial source.

China's archival references to dust storms date back to 1150 BCE and are particularly common in the past millennium. Zhang (1984) found 1156 records of dust palls and was able to discriminate between regional and local events. Ancient records of dust from central Asian and Chinese sources, dating back some 2000 years, have also been found in Korea and Japan. Regular dust storms over the eastern Atlantic have been known for centuries, and Charles Darwin encountered one of them off the Cape Verde island of Santiago in January 1832. Northeasterly *harmattan* winds blew over Africa's west coast, depositing a very fine reddish brown dust on the *Beagle*, reducing visibility to less than two kilometres.

The remarkable Dust Bowl years of the 1930s affected large areas in the central and western USA. Millions of acres of ploughed farmland were exposed to strong winds, creating huge dust storms. This catastrophe was caused by droughts and arguably was exacerbated by poor agricultural practices. In 1938, an estimated 850 million tonnes (Mt) of farmland topsoil were removed.

DUST CHARACTERIZATION

Sampling sites at high elevation, such as at Izaña, Tenerife (2367 m), and Pico de la Gorra, Gran Canaria (1930 m), in the Canary Islands, are well situated to intercept desert plumes on their way from the Sahara and the Sahel to the Caribbean and the Americas. In a similar fashion, the Mauna Loa Observatory, Hawai'i (3394 m), collects dust and industrial pollutants from the east coast of China en route across the Pacific to North America.

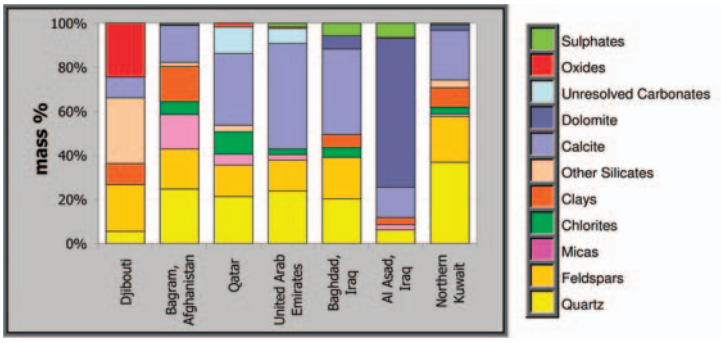

FIGURE 1 Quantitative XRD results for seven <38 µm sieved dust samples from the Middle East. Dust samples are often chemically similar (SEE FIG. 4 TOP) but mineralogically different (Engelbrecht et al. 2009b). The Djibouti sample (African Rift Valley) contains substantial mafic silicate minerals and iron-titanium oxides; the United Arab Emirates and Al Asad samples contain abundant calcite and dolomite, respectively. Kuwaiti samples are rich in silt-sized quartz. Mineralogical differences in regional soils are reflected in the airborne dust transported aloft.

Aerosol monitoring and sampling systems are designed with sampling inlets calibrated to allow passage of specific particle size fractions (e.g. $PM_{2.5}$; see Glossary in Gieré and Querol 2010 this issue), and to collect particulate matter on sampling media for different types of analyses. Improving understanding of the optical properties and biological effects of dust particles requires the merging of chemical, mineralogical and morphological information obtained from optical microscopy, X-ray diffraction (XRD) (FIG. 1), individual-particle electron microscopy, X-ray fluorescence spectrometry, mass spectrometry and other techniques (see Glossary in Gieré and Querol 2010).

Principal components analysis (PCA) and factor analysis (FA) are often applied to chemical data sets of many (>100) samples composed of several chemical species. Positive matrix factorization (PMF) is one FA procedure that has been successfully applied to dust data sets to distinguish amongst source types. For example, PMF values calculated from Greenland ice-core chemical data enabled two factors (source types) to be distinguished: a carbonate-rich source and an aluminous dust profile (Banta et al. 2008).

Chemical data can be compared with measured mineralogical compositions by calculating normative mineral compositions from the chemical results.

DUST SOURCES, PATHWAYS AND FLUXES

Characterization of particulates provides valuable information on dust sources and pathways. The average composition of global dust is dominated by oxides of Si, Al, Fe and Ca, and by carbonates; their proportions are similar to the values for upper continental crust, but overall compositions vary amongst the continents. Some dust and loess deposits in Argentina are poor in quartz and rich in plagioclase, glass shards and other pyroclastic materials because of long-term dust input from Andean volcanoes (Gallet et al. 1998). From its mineralogical and chemical composition, the dust in Antarctic ice is attributed to South American sources (Basile et al. 1997), but may also contain a substantial contribution from east-central Australia (McGowan and Clark 2008).

Grousset and Biscaye (2005) noted that trace element concentrations vary with particle size and that their use in conjunction with other tracers improves the accuracy of dust-source determination. The same is true for the mineralogical composition of dust. Clay minerals, major and minor element ratios, rare earth element (REE) abundances, and Sr, Nd and lead (Pb) isotope ratios can retain their source-specific characteristics during transport (Biscaye et al. 1997). Isotope ratios have become the preferred dust tracer method (Gaiero et al. 2007).

Mean dust particle size declines with distance from source, the finer fractions increasing proportionately (through dry deposition of coarser particles). Particle concentrations decrease as a result of scavenging within clouds and during rainfall events (through wet deposition). These processes affect the mineral content of the dust, the coarser fraction (commonly quartz and feldspars) diminishing as the proportion of finer-grained minerals, such as phyllosilicates and carbonates, increases. The size-dependent processes of deflation at the source and of fractionation during transport and deposition also tend to enhance the trace element contents. The clay fraction eventually dominates composition, such that the background dust has a mean diameter of ≤5 µm. According to Lawrence and Neff (2009), the global background dust depositional rate is of the order of 0.05–1.00 g/m^2/y. The finer fractions of Saharan dust take about one week to reach regions in the Americas as far apart as Florida, the Caribbean islands and northeastern Brazil (Prospero et al. 1981).

Global Dust Flux

Global dust flux varies with the degree of exposure of fine dust particles to surface winds, the frequency of threshold wind velocities, gravitational fallout, the vertical distribution of dust, and the mode of deposition (dry or wet). Estimates are based on relatively sparse in situ (ground-based or in-flight) measurements, orbital satellite data and modelling. Satellite data include aerosol optical thickness or depth, which is a measure of the global attenuation of direct solar radiation (Mahowald et al. 2005), the total ozone mapping spectrometer aerosol index (TOMS AI), and the infrared difference dust index (IDDI). These parameters provide data on dust sources, pathways and depositional locations, but the quantitative extraction of dust properties from them is limited. Thus, depositional estimates based solely on aerosol optical thickness, for example, are uncertain. Despite this difficulty and the problem of discriminating between wet and dry deposition, model results compare moderately well with total deposition measurements. These diverse approaches suggest a global dust flux from all sources of between 1000 and 2150 Tg/y (Andreae and Rosenfeld 2008) (1 Tg = 10^{12} g = 1 Mt), with an estimated mean of 1700 Tg/y (Jickells et al. 2005). Nevertheless, substantial annual variation and extrapolation from relatively few direct measurements lead to varying global estimates. Many published estimates are largely dependent on global dust modelling; values for different source regions differ from one model to the next, giving rise to considerable uncertainty with respect, for example, to determining the relative magnitudes of dust emissions from North Africa and central and eastern Asia (Tegen et al. 2002). Some estimates depend on global models that restrict emissions to clay-size and fine-silt particles (Lawrence and Neff 2009).

Mass fluxes of dust at regional scale may be estimated with greater confidence, although estimates for extensive areas, such as North Africa, vary considerably from 240 ± 80 Tg/y (Koren et al. 2006) to 517–1530 Tg/y (Tanaka and Chiba 2006). Dominant, low-level, easterly winds ('trade winds') drive dust westwards as far as northern South America, reaching a peak from February to April and producing an estimated annual dust fall in the northern Amazon Basin of 13 Tg (Griffin et al. 2001). In summer and early autumn, large amounts of Saharan dust reach the Caribbean, Central America and the southeastern USA (Prospero and Nees 1986). This annual flux was estimated at 130 Tg/y in 1990 and 460 Tg/y in 1991, some 50% of the annual flux occurring during one-fifth of each year (Swap et al. 1996). Dust originating from the diatomite-rich sediments of the formerly much larger Lake Chad in the Bodélé Depression (central Sahara) contributes 1.2 ± 0.4 Tg/d, which is 6 to 18% of global estimates (Todd et al. 2007). In eastern Asia, 30% of the total annual dust mass is redeposited locally, a further 20% accumulates at regional scale, and the remaining 50% enters the global circulation system. A recent numerical study of the global dust budget is based on a global aerosol-transport model, in which the land hemisphere is divided into nine potential dust source regions. Outcomes include estimated Saharan contributions to global emissions and load of 58 wt% and 62 wt%, respectively. This region controls dust distribution over most of the Northern Hemisphere, although values for the Sahara (1087 Tg/y) may be overestimated and those of eastern Asia (146 Tg/y) underestimated (Tanaka and Chiba 2006).

Determining the regional impact, such as soil degradation in dust source areas, is more reliable when based on ground-station data. Measured data exist for notable anthropogenic sources, such as the desiccated Aral Sea basin and Owens Lake, California.

Major Northern Hemisphere Source Regions

North Africa

The West African *harmattan* is a dry and dusty trade wind blowing from the northeast across the Sahara and into the Gulf of Guinea from the end of November to mid-March. Warm, humid air is often drawn from the humid tropical zone to the south, ahead of a cold front or depression north of the Canary Islands. These dust palls, known locally as *calima*, are raised to ~5000 m and may be transported as far as the Caribbean and South America (Goudie and

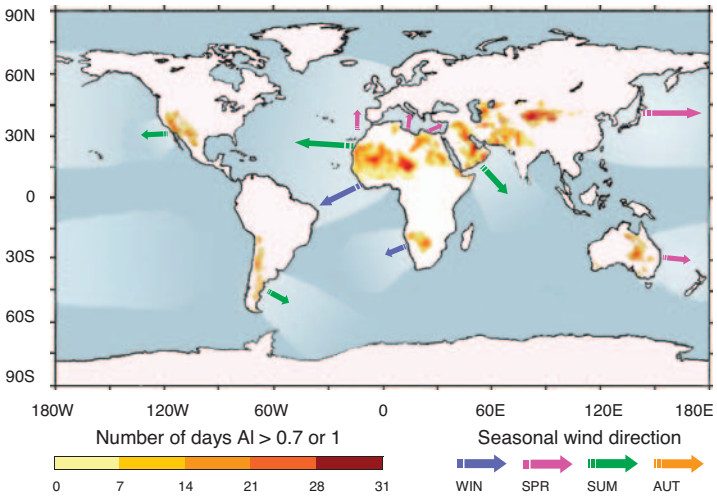

Figure 2 Global distribution of dust sources (after Prospero et al. 2002). The number of days exceeding the absorbing aerosol index (AI) is shown in shades of yellow and brown. Distributions were computed using a threshold AI of 1.0 in the dust belts and 0.7 elsewhere. Note that the seasons are six months apart in the Northern and Southern Hemispheres. Arrows indicate the general direction of dust storms (no significant storms in autumn), and major impacted areas over the ocean are shown in paler shades of blue.

Middleton 2001). In winter, the dust concentration is more intense at middle and low altitudes (<1000 m), although very dense palls may reach higher levels.

Long-range transport of Sahara and Sahel dust follows three main pathways (Fig. 2): westward across the North Atlantic to the Americas on the northeasterly trade winds; northwards to Europe on the *sirocco* (or *scirocco*) and similar winds; and northeastwards by the *sharav* cyclones to the Middle East (Middleton and Goudie 2001). Dust plumes from inland sources, such as the Bodélé Depression, are recharged and diluted with dust from the regions they are migrating across, and they ultimately take on a mineral signature representing several dust sources.

According to Koren et al. (2006), of the 240 ± 80 Tg of dust transported annually from North Africa, a total of 50 ± 15 Tg reaches the Amazon Basin and, of this fraction, 45 ± 6 Tg comes from the Bodélé Depression. It is estimated that 100 ± 20 Tg/y of dust carried by the *sirocco* and similar winds from North Africa contribute to the formation of *terra rossa* soils in southern Europe and the Levant.

Dust samples from the southern and northern Sahara collected in Italy differ in that the former contain more SiO_2 (60.2 versus 56.5 wt%), less MgO (0.8 versus 3.1 wt%) and less CaO (2.3 versus 8.6 wt%); these differences are evidence of carbonate-rich source regions in the northern Sahara (Goudie and Middleton 2001). Entrained mineral dust from the Sahel in northwestern Africa is characterized by a high Fe/Al ratio due to an abundance of ferralitic (iron oxide–rich) soils in that region (Sokolik and Toon 1999). Dust from the northern Sahara contains a variety of clay minerals, commonly chlorite, illite, smectite and palygorskite, with minor kaolinite; this composition points to a variety of source rocks and varying degrees of chemical weathering. In contrast, kaolinite is the dominant clay mineral in dust from the Sahel, including dust derived from the Bodélé Depression.

Middle East

Large desert areas with less than 100 mm/y of precipitation surround the Arabian Sea, forming one of the largest source areas of natural dust. Strong northwesterly *shamal* winds blowing over Iraq, the Persian Gulf states and the Arabian Peninsula often generate large sandstorms that normally last three to five days. During summer, the polar jet stream moves southwards, approaching the subtropical jet stream and forming strong and often dry cold fronts. These conditions create the region's dust storms, which may number 20 to 50 per year and often result in the ambient air quality guideline values being exceeded (Table 1). Similar winds also occur in winter (Fig. 3).

Despite their chemical similarities (e.g. SiO_2, Al_2O_3, and CaO contents), dust samples from various areas in the Middle East do show mineralogical differences (Engelbrecht et al. 2009a) (Figs. 1, 4): samples from the United Arab Emirates and northern Iraq (Al Asad) have slightly higher CaO, MgO and carbonate contents, which are derived locally from carbonate-rich soils in both regions. Sodium generally occurs as salt (NaCl), derived from evaporated sea water and playas. Sulphate, present partly as secondary ammonium sulphate but largely as gypsum, is contained in all samples. Ammonium sulphate is, in all likelihood, derived from sulphur dioxide emitted from petrochemical and other industries in the Gulf region.

Far East

Dust entrainment and transport in Asia are affected by two major atmospheric circulation systems: the Asian monsoon and the westerlies. In winter across northern Eurasia, the Siberian High, a prominent high-pressure system, sustains very cold but stable atmospheric conditions. During spring, however, the Siberian High declines in both stability and size. Cold fronts associated with low-pressure cells and troughs of the westerlies system track along the southern margin of the Siberian High. Vigorous pre-frontal troughs then raise the dust to altitudes ranging from 1 to over 3 km; such strong uplift can inject dust into the jet streams at heights of more than 10 km (Pye 1987). Driven by frontal systems of the westerlies, mineral dust plumes emerge from the drylands of Mongolia and northern China and enter the lower troposphere. Mongolian dust, sometimes transported for thousands of kilometres, gives rise to the severe late-winter and spring dust storms experienced by the megacities of northern, eastern and southern China.

Country	Site	(a) $PM_{2.5}$ $\mu g/m^3$	(b) PM_{10} $\mu g/m^3$	(c) $PM_{2.5}/PM_{10}$ ratios	(d) % Events PM_{10}>150
Djibouti	Djibouti	33	72	0.46	4
Afghanistan	Bagram	40	120	0.34	29
	Khowst	75	126	0.60	36
Qatar	Qatar	67	166	0.41	21
UAE	UAE	52	140	0.37	40
Iraq	Balad	56	183	0.30	74
	Baghdad	103	250	0.42	62
	Tallil	65	303	0.21	56
	Tikrit	114	300	0.38	57
	Taji	81	213	0.38	40
	Al Asad	38	96	0.39	18
Kuwait	North	67	211	0.32	30
	Central	117	298	0.39	33
	Coast	60	180	0.33	42
	South	62	199	0.31	73

Table 1 DATA FOR MIDDLE EAST DUST SAMPLES COLLECTED MOSTLY IN 2006

Columns (a) and (b): annual average particulate mass concentrations; (c): mass ratios of $PM_{2.5}/PM_{10}$; (d): percentage of days when PM_{10} exceeded 150 $\mu g/m^3$ (US EPA National Ambient Air Quality Standard). On average, 43 days were sampled per site (Engelbrecht et al. 2009a). Resilient silicate minerals, such as quartz and feldspars, concentrate in the coarser fraction, whereas finer clay minerals, softer carbonates and combustion products are more abundant in the finer size fraction. Low $PM_{2.5}/PM_{10}$ ratios (<0.4) suggest a high proportion of coarse silicates.

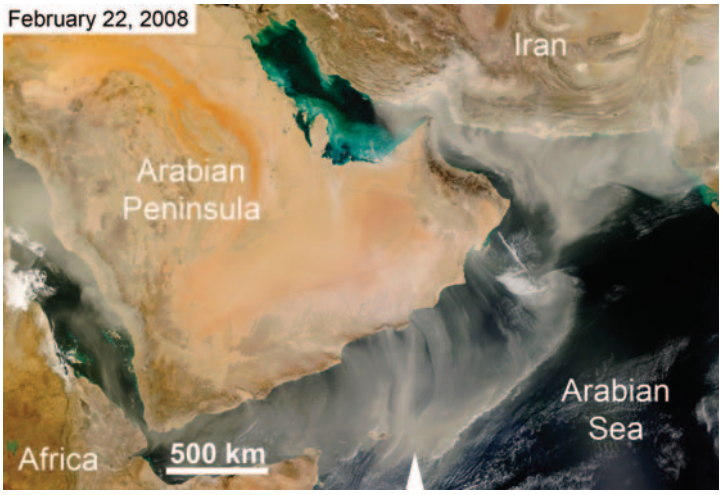

Figure 3 Satellite image of a dust storm, generated by northwesterly *shamal* winds, extending from the horn of Africa to India. Visible dust sheets blow from the Arabian Peninsula, as well as from Iran and Pakistan (top right). Dust streamers extend across the waters of the Red Sea (left), Persian Gulf (centre) and Arabian Sea. Satellite image courtesy of NASA

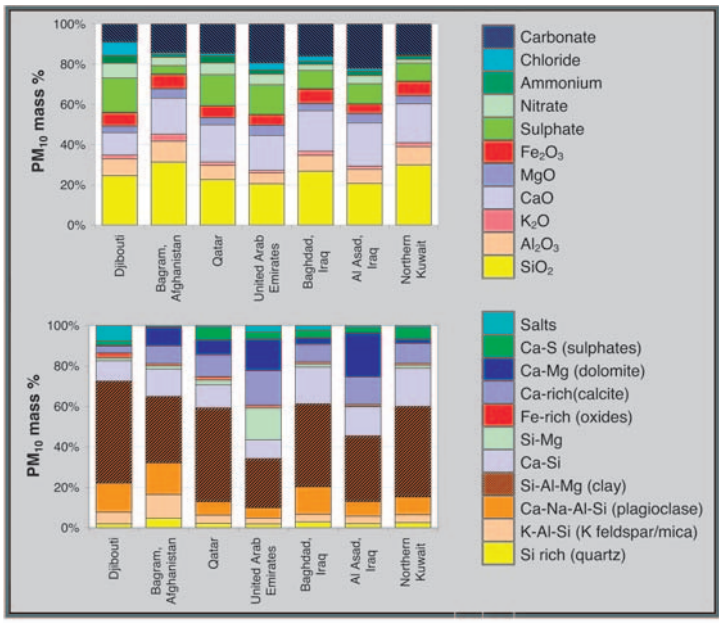

Figure 4 Chemical and electron microscope analyses for Middle East PM_{10} dust sample. (**Top**) Concentrations (in mass %) of oxides, sulphate (in gypsum), chloride (in salt), nitrate, ammonium, and carbonates. (**Bottom**) Elemental compositions obtained by single-particle electron microscopy. Clay (Si–Al–Mg) minerals, generally occurring as coatings on other silicates, form the largest fraction of particles when analyzed by this method (Engelbrecht et al. 2009a).

In western China, the Tarim Basin (containing the Taklamakan Desert) is encircled by the western Kunlun, Pamir and western Tian Shan mountain ranges, all more than 7000 m high. These mountains act as a strong orographic driver, enhancing the pressure gradients along the contact zones between high- and low-pressure cells. This invigorates the frontal systems, raising the desert dust into the westerlies of the upper troposphere (>8 km). Mineral dust derived from both the Mongolian and Taklamakan source regions and transported in the troposphere has been found in ice cores from Greenland (Bory et al. 2003), the finest particles of Taklamakan dust having circled the globe more than once (Uno et al. 2009).

Other Source Areas

Australia

Despite the fact that 85% of the area of Australia is arid, it is a minor source of global dust. However, during the three days following September 22, 2009, a massive dust plume originating in the Lake Eyre Basin (South Australia) swept eastward, reaching a width of about 500 km and a length of nearly 5500 km as it traversed the Tasman Sea to New Zealand. Considered the worst storm in 70 years in New South Wales, its measured particulate concentration levels exceeded 15,000 μg/m^3, in contrast to normal levels of <20 μg/m^3. The Australian research organization CSIRO estimated that 16 Tg of dust was stripped from the central deserts, with up to 75,000 t/h crossing the New South Wales coast north of Sydney. Four days later, another intense storm crossed eastern Australia and entered the Coral Sea, providing iron and other nutrients to phytoplankton along the Great Barrier Reef.

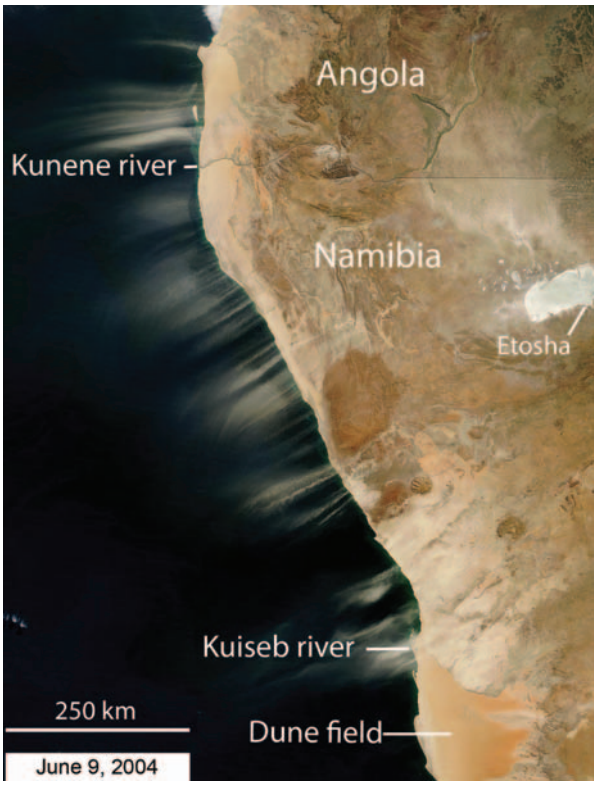

Figure 5 Satellite image of dust plumes streaming westward off the coast of Angola and Namibia. Green hues along the coastline indicate the presence of phytoplankton in surface waters. Note that, due to the coarse nature of sand grains, no dust is coming off the dune field along the southern coastline. Satellite image courtesy of NASA

Southern Africa

Southern Africa's contribution to the global dust budget is small (3 wt%), most of it coming from the western arid regions. The frequent influx of iron-rich desert dust, together with the upwelling of cold, nutrient-rich waters from depth, makes the coastal waters of Namibia and Angola some of the most biologically productive ocean waters on Earth. Point sources of dust correspond to ephemeral river beds, and lesser dust clouds originate at the western edge of the Etosha Pan and in the region further north (Fig. 5).

PERSPECTIVES

The bulk movement of soil due to wind can act as both a degradation process (soil erosion with net nutrient loss) and an enhancement process (supplying nutrients to both terrestrial and marine ecosystems). Substantial advances in global information and in the understanding of the behaviour and effects of airborne dust have been made in the past two or three decades. This gain in knowledge has been made possible by more and better-quality primary data and increasingly sophisticated modelling techniques.

Dust characterization and interpretation demands multi-disciplinary expertise and techniques. The use of an increasingly wide range of dust properties, including mineralogical, elemental and isotopic compositions, has refined the 'finger printing' of both single-grain and bulk dust samples. These techniques promise further advances at both regional and global scales, although standardized data and metrics to facilitate improved comparative global studies are needed.

ACKNOWLEDGMENTS

The authors thank Greta Engelbrecht for drafting the figures and the table for this publication. This manuscript benefitted greatly from comments by Taichu Tanaka, four anonymous reviewers, and editors David Vaughan and Reto Gieré.

REFERENCES

Andreae MO, Rosenfeld D (2008) Aerosol–cloud–precipitation interactions. Part 1. The nature and sources of cloud-active aerosols. Earth-Science Reviews 89: 13-41

Banta JR, McConnell JR, Edwards R, Engelbrecht JP (2008) Delineation of carbonate dust, aluminous dust, and sea salt deposition in a Greenland glacio-chemical array using positive matrix factorization. Geochemistry Geophysics Geosystems 9: Q07013, doi:10.01029/2007GC001908

Basile I, Grousset FE, Revel M, Petit JR, Biscaye PE, Barkov NI (1997) Patagonian origin of glacial dust deposited in East Antarctica (Vostok and Dome C) during glacial stages 2, 4 and 6. Earth and Planetary Science Letters 146: 573-589

Biscaye PE, Grousset FE, Revel M, Van der Gaast S, Zielinski GA, Vaars A, Kukla G (1997) Asian provenance of glacial dust (stage 2) in the Greenland Ice Sheet Project 2 Ice Core, Summit, Greenland. Journal of Geophysical Research 102: 26765-26781

Bory AJM, Biscaye PE, Grousset FE (2003) Two distinct seasonal Asian source regions for mineral dust deposited in Greenland (NorthGRIP). Geophysical Research Letters 30: 1167, doi:10.1029/2002GL016446

Derbyshire E, Meng X, Kemp RA (1998) Provenance, transport and characteristics of modern aeolian dust in western Gansu Province, China, and interpretation of the Quaternary loess record. Journal of Arid Environments 39: 497-516

Engelbrecht JP, McDonald EV, Gillies JA, Jayanty RKM, Casuccio G, Gertler AW (2009a) Characterizing mineral dusts and other aerosols from the Middle East —Part 1: Ambient sampling. Inhalation Toxicology 21: 297-326

Engelbrecht JP, McDonald EV, Gillies JA, Jayanty RKM, Casuccio G, Gertler AW (2009b) Characterizing mineral dusts and other aerosols from the Middle East—Part 2: Grab samples and re-suspensions. Inhalation Toxicology 21: 327-336

EPICA community members (2004) Eight glacial cycles from an Antarctic ice core. Nature 429: 623-628

Gaiero DM, Brunet F, Probst J-L, Depetris PJ (2007) A uniform isotopic and chemical signature of dust exported from Patagonia: Rock sources and occurrence in southern environments. Chemical Geology 238: 107-120

Gallet S, Jahn B, Van Vliet Lanoë B, Dia A, Rossello E (1998) Loess geochemistry and its implications for particle origin and composition of the upper continental crust. Earth and Planetary Science Letters 156: 157-172

Gieré R, Querol X (2010) Solid particulate matter in the atmosphere. Elements 6: 215-222

Ginoux P, Garbuzov D, Hsu NC (2010) Identification of anthropogenic and natural dust sources using Moderate Resolution Imaging Spectroradiometer (MODIS) Deep Blue level 2 data. Journal of Geophysical Research 115: D05204, doi:10.1029/2009JD012398

Goudie AS, Middleton NJ (2001) Saharan dust storms: nature and consequences Earth-Science Reviews 56: 179-204

Griffin DW (2007) Atmospheric movement of microorganisms in clouds of desert dust and implications for human health. Clinical Microbiology Reviews 20: 459-477

Griffin DW, Garrison VH, Herman JR, Shinn EA (2001) African desert dust in the Caribbean atmosphere: Microbiology and public health. Aerobiologia 17: 203-213

Grousset FE, Biscaye PE (2005) Tracing dust sources and transport patterns using Sr, Nd and Pb isotopes. Chemical Geology 222: 149-167

Jickells TD, Dorling S, Deuser WG, Church TM, Arimoto R, Prospero JM (1998) Air-borne dust fluxes to a deep water sediment trap in the Sargossa Sea. Global Biogeochemical Cycles 12: 311-320

Jickells TD and 18 coauthors (2005) Global iron connections between desert dust, ocean biogeochemistry, and climate. Science 308: 67-71

Kohfeld KE, Harrison SP (2003) Glacial-interglacial changes in dust deposition on the Chinese Loess Plateau. Quaternary Science Reviews 22: 1859-1878

Koren I, Kaufman YJ, Washington R, Todd MC, Rudich Y, Martins JV, Rosenfeld D (2006) The Bodélé Depression: a single spot in the Sahara that provides most of the mineral dust to the Amazon forest. Environmental Research Letters 1: 014005, doi:10.1088/1748/1748-9326/1/1!014005

Lawrence CR, Neff JC (2009) The contemporary physical and chemical flux of aeolian dust: A synthesis of direct measurements of dust deposition. Chemical Geology 267: 46-63

Li G, Chen J, Ji J, Yang J, Conway TM (2009) Natural and anthropogenic sources of East Asian dust. Geology 37: 727-730

Mahowald NM, Baker AR, Bergametti G, Brooks N, Duce RA, Jickells TD, Kubilay N, Prospero JM, Tegen I (2005) Atmospheric global dust cycle and iron inputs to the ocean. Global Biogeochemical Cycles 19: GB4025, doi: 10.1029/2004GB002402

McGowan HA, Clark A (2008) A vertical profile of PM10 dust concentrations measured during a regional dust event identified by MODIS Terra, western Queensland, Australia. Journal of Geophysical Research 113: F02803, doi:10.1029/2007JF000765

Middleton NJ, Goudie AS (2001) Saharan dust: Sources and trajectories. Transactions of the Institute of British Geographers, New Series 26: 165-181

Prospero JM (1999) Long-range transport of mineral dust in the global atmosphere: Impact of African dust on the environment of the southeastern United States. Proceedings of the National Academy of Sciences 96: 3396-3403

Prospero JM, Nees RT (1986) Impact of the North African drought and El Niño on mineral dust in the Barbados trade winds. Nature 320: 735-738

Prospero JM, Glaccum RA, Nees RT (1981) Atmospheric transport of soil dust from Africa to South America. Nature 289: 570-572

Prospero JM, Ginoux P, Torres O, Nicholson SE, Gill TE (2002) Environmental characterization of global sources of atmospheric soil dust identified with the NIMBUS 7 Total Ozone Mapping Spectrometer (TOMS) absorbing aerosol product. Reviews of Geophysics 40: 1002, doi: 10.1029/2000RG000095

Pye K (1987) Aeolian Dust and Dust Deposits. Academic Press, London, 312 pp

Sokolik IN, Toon OB (1999) Incorporation of mineralogical composition into models of the radiative properties of mineral aerosol from UV to IR wavelengths. Journal of Geophysical Research 104(D): 9423-9444

Sun J, Kohfeld KE, Harrison SP (2000) Records of Aeolian Dust Deposition on the Chinese Loess Plateau during the Late Quaternary. Technical Report Max Planck Institute for Biochemistry, Jena, Germany, 318 pp

Swap R, Ulanski S, Cobbett M, Garstang M (1996) Temporal and spatial characteristics of Saharan dust outbreaks. Journal of Geophysical Research 101(D2): 4205-4220

Tanaka TY, Chiba M (2006) A numerical study of the contributions of dust source regions to the global dust budget. Global and Planetary Change 52: 88-104

Tegen I, Harrison SP, Kohfeld K, Prentice IC, Coe M, Heimann M (2002) Impact of vegetation and preferential source areas on global dust aerosol: Results from a model study. Journal of Geophysical Research 107 (D21): 4576, doi: 10.1029/2001JD000963

Todd MC, Washington R, Martins JV, Dubovik O, Lizcano G, M'Bainayel S, Engelstaedter S (2007) Mineral dust emission from the Bodélé Depression, Chad during BoDEx. 2005. Journal of Geophysical Research 112: D06207, doi:10.1029/2006JD007170

Uno I, Eguchi K, Yumimoto K, Takemura T, Shimizu A, Uematsu M, Liu Z, Wang Z, Hara Y, Sugimoto N (2009) Asian dust transported one full circuit around the globe. Nature Geoscience 2: 557-560

Zhang D (1984) A preliminary analysis of synoptic climatology of falling dust since the historical period in China. Scientia Sinica Serie B 3: 278-288, 825-836